International Journal for Multidisciplinary Research (IJFMR)
E-ISSN: 2582-2160 ● Website: www.ijfmr.com ● Email: editor@ijfmr.com

Multi-Decadal Assessment of Land Use Land Cover Change and Its Impacts on Vegetation, Built-up Expansion, and Land Surface Temperature Using Remote Sensing and GIS

Mr. Kalobaran Das[1], Dr. Rabindra Nath Ray[2]

[1]Research Scholar, Department of Geography, Magadh University, Bodhgaya, Bihar
[2]Associate Professor, Department of Geography, S.B.A.N. College, Darheta - Lari

Abstract:
The LULC changes have an important effect on the vegetation, the growth of built-up, and the land surface temperature (LST), especially in rapidly evolving coastal and agrarian landscapes. This paper is a multi-decadal evaluation (1991-2021) of LULC dynamics and its environmental consequences in Purba Medinipur district in West Bengal in India, based on multi-temporal Landsat, and Google Earth engine. LULC maps were created using supervised classification and NDVI, NDBI, and LST were created to assess vegetation health, urban growth, and thermal features. Assessments of accuracy showed good reliability of classification with an overall accuracy of over 89 percent and a Kappa value of approximately 0.87 to 0.88 among all the benchmark years. Findings indicate that the percentage of cropland fell gradually in 93.37% (1991) to 90.20% in 2021, with built-up areas steadily growing by 1.93 percent up to 2.77 percent. Classes of wetlands including marsh land and tidal flat had varying and generally decreasing tendencies, whereas water bodies recorded a significant rise in 2021. Due to the analysis of NDVI, high and very high vegetation classes were significantly reduced and low and very low vegetation classes were significantly increased because the anthropogenic pressure and stress on vegetation were increasing. At the same time, LST trends show that the surface heating is becoming more and more intense as the highest temperatures increase to 37.63 in 1991, and to more than 43 in 2021, and cooler areas are becoming more and more fractured. The multi-index analysis shows that there is a strong relationship between the spatial vegetation degradation, built-up expansion, wetland transformation and thermal intensification. The results highlight the long-term effects of urbanization and agricultural intensification and coastal environmental alteration as well on landscape sustainability. The research is very useful in climate resilience planning, sustainable land management and conservation of the ecology of vulnerable coastal districts.

Keywords: Land Use Land Cover (LULC) Change, Land Surface Temperature (LST), Normalized Difference Vegetation Index (NDVI), Normalized Difference Built-up Index (NDBI), Urbanization and Vegetation Dynamics

1.0 Introduction:

The land use land cover dynamics are very important in determining the thermal and ecological features

of the Earth surface especially in fast changing coastal and agrarian areas(Acharya et al., 2023). Changes in land cover have a direct effect on the essential biophysical attributes of surfaces, including albedo, surface roughness, emissivity, and surface moisture, and affect the thermodynamics of surfaces(Juhadi et al., 2021). These changes have a strong influence at land surface temperature patterns, distribution of vegetation and ecosystem functioning. The unceasing conversion of land has been enhanced by the increasing population in most developing areas, the growing needs of food and other resources and the increase in developmental activities(Dolui and Sarkar, 2024). Consequently, there is an increasing imbalance between the natural ecosystems and anthropogenic land use systems. Vegetated and wetland landscapes are often fractured with the growth of settlements and road systems and other infrastructures. These alterations decrease the potential of evapotranspiration and increase the surface heating by increasing the sensible heat flux. Therefore, knowing the land use land cover changes is crucial to environmental sustainability, climate resilience and long-term resource planning. Such changes are monitored and interpreted to give insightful information in regard to how the landscape reacts to human pressures as well as the environmental stressors. Hence, systematic evaluation of the land transformational processes is needed in determination of the critical areas of ecological degradation and thermal stress both in space and time(Putri et al., 2020).

The geospatial and remote sensing methods offer effective, consistent and economical methods of measuring multi temporal changes in land use land cover and the environmental impacts. The satellite derived indices find extensive use in assessing surface property of the land and how it changes spatiotemporally and at varied scale(Acharya et al., 2023; Dolui and Sarkar, 2024; Putri et al., 2020). Land surface temperature is also a major indicator of the thermal state of the surface and indicates land cover composition as well as climatic variability. Similarly, normalized difference vegetation index is normally employed to quantify vegetation greenness, health, availability of biomass and productivity hence reflects the vegetation response to environmental changes. Besides, the normalized difference built up index has also been discovered to be useful in the detection of built-up surfaces as well as monitoring urban expansion by differentiating the impervious features of the land to vegetation and soil. These indices, coupled with classified land use land cover maps, provide an in-depth perspective of both surface conditions and surface transitions. Multi temporal satellite data make certain that there is consistent and spatially explicit assessment over extended time periods, which allow the assessment of gradual and abrupt changes in the land(Setturu et al., 2010). The integration aids the improved perception of surface temperatures in the context of vegetation variations and constructed growth. Besides, these assessments enable the detection of spatial hotspots in which the environmental stress is rising at an alarming rate. Therefore, the methods of remote sensing have become ideal tools of observing landscape changes and have been integrated in evidence-based planning of climate adaptation and sustainable land management(Roy and Kasemi, 2021).

Though there is widespread literature on land use land cover change and environmental indices, some of the limitations are still apparent in the literature with regard to the long-term regional scale studies. Most of the previous studies concentrated on a single parameter like the NDVI based vegetation assessment or LST based thermal mapping, and did not combine multiple indicators to indicate the joint environmental response (Keerthi Naidu & Chundeli, 2023). The urban heat island research in many instances favours urban built-up developments but does not directly relate thermal patterns with vegetation responses and land use change in the adjacent rural environments (Sarkar et al., 2025; Shahfahad et al., 2020). Likewise, vegetation change research frequently presents the decline in greenness or enhancement and

fails to sufficiently demonstrate the role settlement increase and surface alteration in supporting the observed patterns. The other significant limitation is that most studies are limited in terms of the time span, most studies are limited to a short time span hence missing long term cumulative effects and multi decadal environmental changes. In coastal and deltaic areas, where the geomorphological processes, wetlands dynamics, and salinity variations have a strong impact on land cover, the combined effects of land transformation and the variation in hydrology on thermal conditions are usually neglected in the past literature. Also, a number of the studies give qualitative description of spatial changes but do not provide quantitative assessment of area based that can substantiate the level and the proportional contribution of each class. Fewer studies, comparatively speaking, utilize a year-by-year cumulative scheme in which land use land cover changes are linked to surface indices using a number of decades. These constraints limit in-depth knowledge of land transformation drivers and limit the ability to determine high degradation regions. Thus, the gap in the research still needs to be addressed by the integrated multi-index evaluation with the help of quantitative land cover assessment(Ashwini & Sil, 2022; Sarif et al., 2023) .

In order to address these limitations, this study will focus on studying the spatiotemporal variation in land surface temperature, vegetation status, built up growth, and land use land cover change with a span of multi decadal period (Guha & Govil, 2021). The analysis aims at determining variations of annual years as selected benchmark years in order to isolate the long-term variations and spatial variations in surface attributes. Particularly, the study aims at quantifying land use land cover classes and calculating their changes in area and percentage over a period of time to determine major pathways of land transformation. At the same time, the goal of the study is to determine the changes in the NDVI classes to evaluate the variations in vegetation health and density, correlate these dynamics with the land transformation processes (Panigrahi and Sharma, 2025). The other key objective is to analyse the built-up expansion based on the NDBI based mapping and analysing its spatial growth pattern between the scattered settlements to the clustered urban forms. Moreover, the paper will seek to perceive the overall effect of these land use modifications and vegetation shifts, and built up growth on the thermal condition signalled in the land surface temperature maps. The research tries to bring out the spatial relationships between vegetation degradation, the growing impervious areas, and the rise in temperature zones by combining these datasets. The research also seeks to find the hotspot areas where fast land change is causing ecological pressure and temperature increment. In the end, these objectives assist in enhancing the comprehension of how the landscape is changing and its effects on environmental sustainability and climate susceptibility (Mukherjee, 2022; Pathak et al., 2021).

This study has been characterized by novelty in that it has fully incorporated LST, NDVI, NDBI, and a clear land use land cover classification in a consistent year wise analysis. This study provides a close relationship between land transformation patterns and surface thermal ecological responses across several decades unlike most of the earlier studies which discuss these parameters separately. The year wise methodology will facilitate the identification of both slow changes and significant shifts in the level of environmental change and therefore gives a better picture of the cumulative effects. Additionally, the analysis integrates the spatial mapping with the quantitative analysis of areas in percentages and percentage, which allows the study to conduct the analysis of the land cover and index class dynamics both through the visual interpretation and statistical comparison. Multi index assessment enhances reliability of interpretation since it cross validates changes in vegetation and built-up with their thermal impacts. This combined approach is especially effective in coastal and agricultural settings where the

land cover change processes are complicated, and they depend on human and natural processes. Moreover, the research has a value of determining spatial hot spots of thermal stress and vegetation degradation that are associated with built up growth and the change in wetlands. The results provide policy formulation, sustainable development of land use, ecosystem protection, and climate change adaptation facilities. Hence, the multi decadal analysis that has been integrated in this work gives a new and strong contribution in the understanding of the induced environmental change by human being and its thermal ecological implications.

2.0 Materials and method:

2.1 Data source:

This paper used multi temporal Landsat satellite data to extract the Land Surface Temperature, NDVI, NDBI and LULC maps between 1991 and 2021. The historical years mostly used were 19912011 with Landsat 5 TM Collection 2 Level 2 products, which were LANDSAT/LT05/C02/T1L2 and the recent years 2013 2021 with Landsat 8 OLI/TIRS Collection 2 Level 2 products. These Level 2 datasets include atmospherically corrected surface reflectance bands of vegetation indices and land cover classification and surface temperature bands of LST estimation. All images had been spatially filtered using the study area boundary ROI, and temporally by annual or selected benchmark year date ranges. The bitwise masking of the cloud and cloud shadow pixels with the help of the QA_PIXEL band and further filtering on the basis of cloud cover threshold as needed was applied. Analysis and processing were performed in Google Earth Engine to provide the same preprocessing, annual composite generation, and export of results as GeoTIFF in 30 m spatial resolution (Sreenivasulu and Udaya Bhaskar, 2010).

2.2 LULC :

Preparation of land use land cover mapping was done by use of Landsat surface reflectance composite images that were done with supervised classification. Cloud filtered Landsat images were created to create a median composite raster of the typical spectral conditions at that time during each target year. The composite was cut to ROI and reflectance bands SRB1, SRB2, SRB3, SRB4, SRB5 and SRB7 were used as inputs in classification. Field knowledge and reference interpretation were used to collect training samples of the major land cover classes of agriculture, vegetation, water, built up and barren land. Spectral signatures were extracted with the sample Regions function of the merged training data to create a training table of the classifier model development (Roy and Kasemi, 2021).

2.3 NDBI:

Normalized Difference Built up Index was developed to track the expansion and impervious surfaces of built ups using the Landsat surface reflectance data. The Landsat collections were filtered according to study boundary, and time periods in which the target year was chosen. The Landsat scaling factors were used to scale surface reflectance bands to normalize digital values into valid reflectance bands before computing NDBI (Thapa et al., 2023). NDBI was calculated on each cloud free scene and annual averages were determined on NDBI values of the target years (1991, 2001, 2011, and 2021). This composite method is an annual one that eliminates scene specific outliers and gives representative patterns of built ups per year. All the Annual NDBI rasters were clipped to ROI to have a uniform spatial boundary.

NDBI calculation was based on the normalized difference equation NDBI = (SWIR -NIR)/(SWIR + NIR). In the case of Landsat 5, the NDBI = (SR B5- SR B4)/ (SR B5 + SR B4), where SR B5 and SR B4

are the SWIR and NIR respectively(Govil et al., 2019; Kumar & Singh, 2025). In the case of Landsat 8, NDBI = (SR B6 -SR B5)/(SR B6 + SR B5) with SR B6 indicating SWIR and SR B5 indicating NIR. Positive NDBI values were considered to be built up surfaces whereas a negative value was that which was predominantly vegetation or water.

2.4 NDVI

Normalized Difference Vegetation Index was calculated using Landsat surface reflectance datasets by means of spatial, temporal, and cloud filtering(Sharma et al., 2024). Near Infrared and Red bands were taken as Landsat 5 TM reflectance bands SR_B4 and SR_B3 respectively and Near Infrared and Red as Landsat 8 OLI bands SR_B5 and SR_B4 respectively. QA_PIXEL was used to perform cloud masking to eliminate poor quality pixels and annual NDVI composites were created by averaging all the NDVI layers in each year. This is because the annual mean composite approach means that the results of NDVI give a picture of the stable vegetation condition to make the least of short term seasonal variations and cloud contamination (Tiwari et al., 2025). The NDVI rasters were clipped to ROI every year to ensure that the geographic coverage was the same year after year with a view of making comparisons.

The standard normalized difference formula was used to calculate the NDVI NDVI = (NIR - Red)/(NIR + Red). In the case of Landsat 5, NDVI = (SR (B4) - SR (B3)) / (SR (B4) + SR (B3)).

and for Landsat 8, NDVI = (SR (B5) -SR (B4))/ (SR (B5) + SR (B4)) (Martinez & Labib, 2023). To measure the changes in greenness condition, the values of NDVI were then classified as very low, low, moderate, high, and very high vegetation condition (Martinez & Labib, 2023). NDVI spatial distribution was also interpreted to detect stress and degradation areas of vegetation.

2.5 LST:

Surface Temperature was retrieved on the Landsat Collection 2 Level 2 Surface Temperature products with the following ST: B6 Landsat TM product, and ST: B10 Landsat OLI/TIRS product. The Landsat image collections were initially spatially filtered with ROI boundary and temporally filtered with annual time windows. The QA_PIXEL band was used to remove cloud and cloud shadow pixels by masking with bitwise and only reliable pixels were analyzed. To obtain the annual mean composite of all cloud free scenes, all cloud free scenes were pooled together on a yearly basis to eliminate seasonal noise and to provide stable interannual comparison in the long term. Clipping of the LST images to the ROI finally finished to have the same spatial extent of the images throughout the whole years(Dapke et al., 2025; Sharma et al., 2024).

The raw ST band values were transformed into land surface temperature in Celsius using metadata scale factor and offset of Landsat(S et al., 2024). The conversion equation that can be used in the present study can be represented as LST (o C) = (ST 0.00341802 + 149.0)-273.15 where ST is the value of the surface temperature band (ST B6 in the case of Landsat 5 and ST B10 in the case of Landsat 8). In this operation the band is changed to Kelvin and then to Celsius. The annual LST layers generated were stored under the property year and visualised using a thermal palette to determine hot spots and cool areas(Tiwari et al., 2025).

2.5 Study area:

The Purba Medinipur district is located in the south of West Bengal, India and it occupies a significant coastal district in the Bay of Bengal(Sharmita Ghorai (Maity) et al., 2024). The district is spatially located between 21 30 N and 22 30 N latitude and 87 00 E and 88 00 E longitude as indicated in the location map (Figure 1). The district is located in the lower Gangetic plain and is a transitory zone between alluvial plains inland and deltaic coastal environment(Gayen et al., 2020). It is predominantly

flat and gently undulating in physiography with large depositional landforms within it formed due to processes of fluvial and marine origin. The drains serve the region through various big and small rivers and tidal routes that have a very strong influence on the landform and the hydrological regime, such as the Rupnarayan and Haldi river systems. It has a tropical monsoon climate with hot humid summers, moderate winters, as well as, high levels of rainfall during the south west monsoon. The area is highly susceptible to climatic hazards and environmental pressure due to its location behind the coastal environment that is often susceptible to cyclones, storm surge, seasonal floods, and coastal erosion (Chakraborty et al., 2020).

Agricultural land dominating the land use plan, the Purba Medinipur land use structure is dominated by urban and semi urban settlements along administrative, commercial, and transport corridors. The district has a diverse ecological setting comprising of croplands and wetlands, riverine belts, tidal flats and coastal sandy belts. The patches of natural vegetation are small yet have a significant contribution to the control of microclimate and ecological stability, particularly in the regions that are low lying and affected by water. The persistent increase in population, expansion of infrastructures and transformation of wetlands into built up areas and aquaculture farms have greatly altered the scenery of the district within the past decades. Also, processes in the coastal environment like intrusion of salt and alteration of the shoreline affect the intensity of cropping, the state of vegetation and the availability of surface moisture. The combination of these factors leads to spatial differences in the land surface temperature, the health of the vegetation and built-up expansion in various blocks of the district. Thus, Purba Medinipur will offer an appropriate geographical context to study the long-term land change and its impact on thermal and ecological processes to facilitate the planning of climate resilience and sustainable coastal management in the future(Gayen et al., 2022).

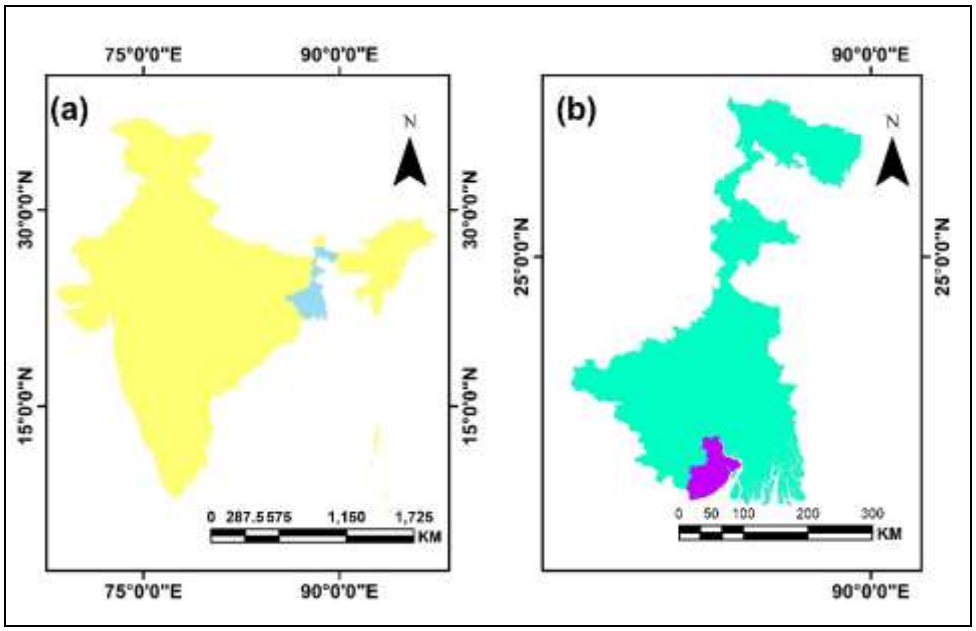

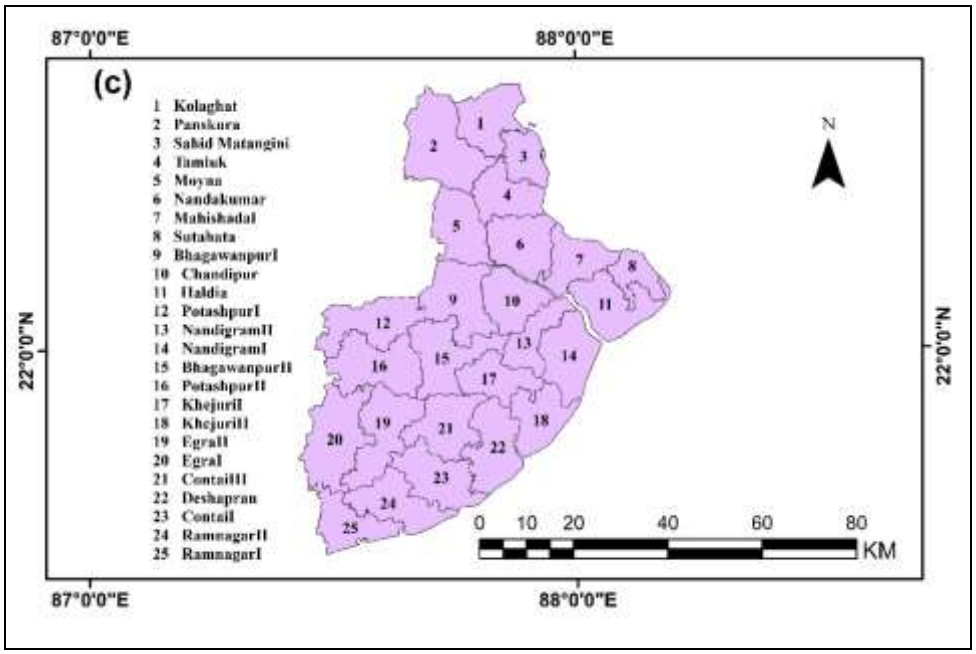

Figure 1: Location of the study area in three levels: (a) map of India indicating the position of West Bengal, (b) map of West Bengal highlighting the Purba Medinipur district, and (c) block wise administrative map of Purba Medinipur district

3.0 Result and discussion:

3.1 LULC: The land use land cover structure of the study area in the year 1991 is heavily comprised of the cropland, about 36,426.65 km 2 of which occupies nearly 93.37 percent of the total study area. This is a clear indication that the major land use activity at this time was agriculture. The vegetation area covers about 664.79 km 2 or 1.70 percent, which is little forest or thick green cover. With an area of 751.42 km 2 (contributing to 1.93 percent) it implies low but established human settlements. The category of wetland related classes including marsh land, tidal flat, flooded flat land, and water bodies take up a small but significant part of land 267.28 km 2 (0.69 percent). Minor proportions of about less than 0.10 percent are held by shrub land, mangrove and salt marsh. Unproductive land covers 138.64 km 2 or 0.36 percent. In general, the 1991 landscape indicates a stable agrarian regime containing very little urbanization and quite preserved coastal and wetlands characteristics (Figure 2).

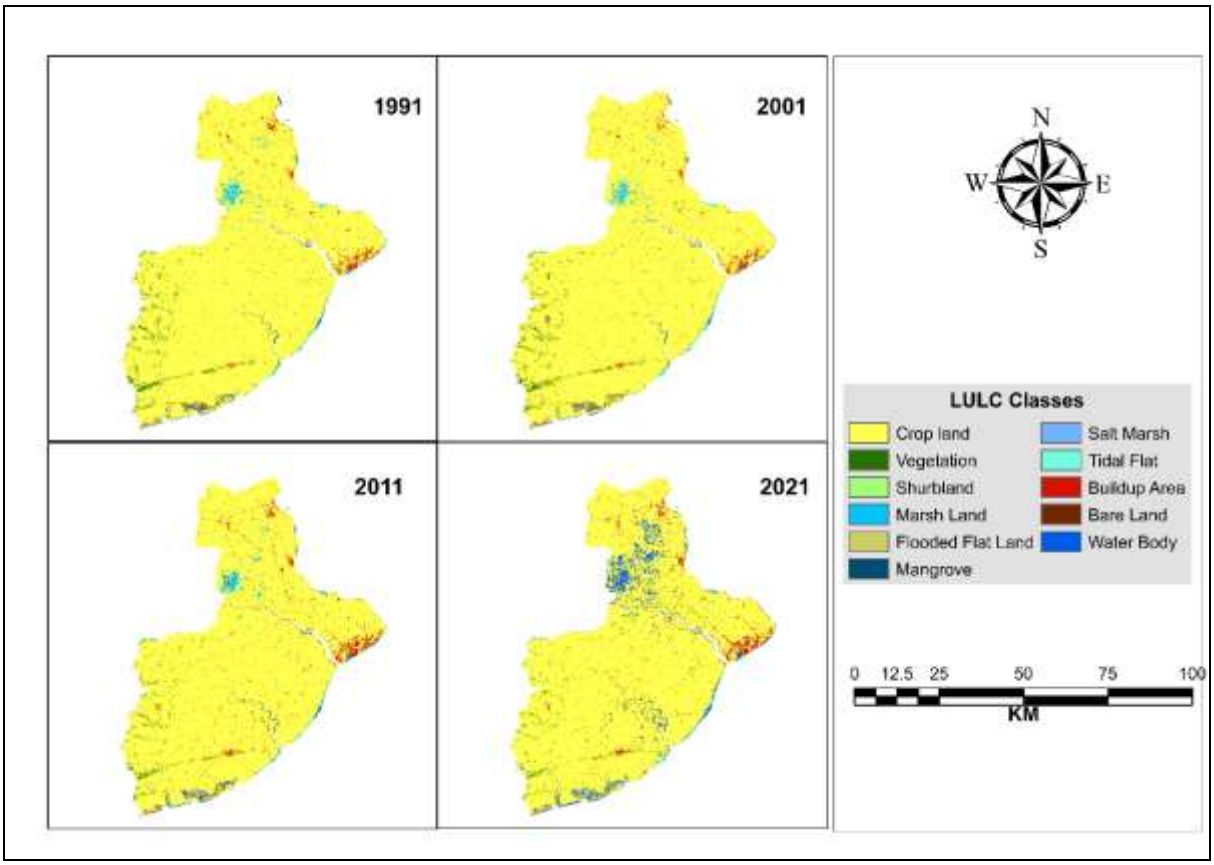

Figure 2: Spatiotemporal land use land cover (LULC) maps of Purba Medinipur district for 1991, 2001, 2011 and 2021.

In 2001, the prevailing class was the cropland, which slightly rose to 36,475.39 km 2 and 93.49 percent of the total, which means that it relied on agriculture. The plant cover is characterized by a peripheral decrease to 655.48 km 2 or 1.68 percent which is an indication of slow strain on the natural greenery. Construction land has stayed almost the same at 751.68 km 2 (1.93 percent), which indicates that urbanization was slow this decade. The area covered by marsh land reduces to 280.26 km2 (0.72 percent) and flooded flat land expands to 196.07km 2 (0.50 percent) perhaps due to drainage or flood dynamics. Tidal flats drop slightly to 238.93 km 2 (0.61 percent) and water bodies drop to 229.91 km 2 (0.59 percent). Mangrove area reduces to 3.74 km 2 whereas salt marsh increases slightly to 10.00 km 2. This has subtle changes which denote the onset of environmental stress, as the general structure of land use remains mostly unchanged (Figure 2).

Table 1: Spatiotemporal Distribution of Land Use/Land Cover (LULC) Classes in Purba Medinipur District (1991–2021) showing Area and Percentage (%)

Class Value	LULC Type	1991		2001		2011		2021	
		Area	% of Area	Area	% of Area	Area	% of Area	Area	% of Area
1	Crop land	36426.65	93.37	36475.39	93.49	36244.43	92.90	35193.05	90.20
2	Vegetation	664.79	1.70	655.48	1.68	533.28	1.37	561.37	1.44
3	Shrub land	40.51	0.10	40.43	0.10	44.30	0.11	38.41	0.10

4	Marsh land	324.60	0.83	280.26	0.72	299.21	0.77	125.82	0.32
5	Flooded flat land	153.39	0.39	196.07	0.50	169.76	0.44	235.49	0.60
6	Mangrove	5.30	0.01	3.74	0.01	2.60	0.01	5.87	0.02
7	Salt marsh	2.16	0.01	10.00	0.03	42.73	0.11	66.76	0.17
8	Tidal flat	240.24	0.62	238.93	0.61	210.14	0.54	163.13	0.42
9	Buildup area	751.42	1.93	751.68	1.93	1016.93	2.61	1079.54	2.77
10	Barren land	138.64	0.36	133.07	0.34	128.39	0.33	146.03	0.37
11	Water body	267.28	0.69	229.91	0.59	323.20	0.83	1399.48	3.59

In 2011, we can see the signs of changes within various categories of LULC. The area area reduces to 36,244.43 km 2 covering 92.90 percent of the land, which means that agricultural land is gradually being converted into cropland. The vegetation reduces more drastically to 533.28 km 2 or 1.37 percent indicating more land degradation or clearing. The built up area rises remarkably to 1,016.93 km 2 which is 2.61 percent, which depicts growing urbanization and development of the infrastructure. Marsh land is slightly recovered to a space of 299.21 km 2 (0.77 percent) and the flooded flat land reduces to 169.76 km 2 (0.44 percent). Salt marsh spreads significantly to 42.73 km 2(0.11 percent), which could be as a result of intrusion of coastal salinity. Tidal flats shrink to 210.14km 2 (0.54 percent). The water bodies expand to 323.20 km 2 (0.83 percent), which means that there are changes in the distribution of surface water. It is a significant shift to a more humanized coastline and human dynamics (Table 1).

The changes that can be seen in the LULC pattern are the strongest changes that took place during the period of study. The Cropland decreases significantly to 35,193.05 km 2, which occupies 90.20 percent of the land, and it is a fact that there is continuous degradation in agricultural land. Built up area also goes up to 1,079.54 km 2 or 2.77 percent, highlighting further urban growth. There is a drastic increase of water bodies to 1,399.48 km 2 which is 3.59 percent showing significant hydrological alterations, like flooding, aquaculture development, or river broadening. The loss of wetland is seen in the shrunken areas of marsh land to 125.82 km 2 (0.32 percent) and tidal flat to 163.13 km 2 (0.42 percent). Flood plain land area grows to 235.49 km 2 (0.60 percent) and salt marsh to 66.76 km 2 (0.17 percent). Mangrove area records slight recovery to 5.87 km 2. These developments point to intensified environmental stress and land change (Table 1).

Altogether, the temporal study of the 1991 to 2021 period demonstrates the slow yet steady change of patterns of land use land cover. Although cropland is still the predominant land type during the period of study, the area and the percentage of the land steadily decrease, which suggests an increase in the pressure of urbanization and changing hydrology. The areas under development are gradually growing, as demonstrated by the presence of built up areas which is an indication of population growth. Wetland and coastal classes (marsh land, tidal flat, and mangrove) have fluctuating trends, which indicate dynamic coastal processes and human interventions. This abrupt rise in water bodies in 2021 indicates a probable high impact of the environment or climate in the last couple of years. All these trends demonstrate a shift in a rather stable agricultural environment to the more complex and human altered land use system over a period of thirty years.

Table2: Accuracy assessment of LULC 1991													
LULC class	Crop land	Vegetation	Shrub land	Marsh land	Flooded flat land	Mangrove	Salt marsh	Tidal flat	Buildup area	Barren land	Water body	Total (User)	User Accuracy (%)
Crop land	173	4	7	0	2	0	0	0	0	0	0	186	93.01
Vegetation	3	90	0	4	0	0	0	0	0	0	0	97	92.78
Shrub land	0	3	27	0	0	0	0	0	0	0	0	30	90.00
Marsh land	0	0	1	23	0	0	0	0	0	0	0	24	95.83
Flooded flat land	2	0	0	0	13	0	1	0	0	0	0	16	81.25
Mangrove	0	0	0	1	0	5	0	0	0	0	0	6	83.33
Salt marsh	0	0	0	1	0	0	6	0	0	0	0	7	85.71
Tidal flat	0	0	0	0	0	0	0	6	0		2	8	75.00
Buildup area	0	0	0	0	0	0	0	0	50	11	0	61	81.97
Barren land	0	0	0	0	1	0	0	0	4	20	0	25	80.00
Water body	0	0	0	1	0	0	0	0	0	0	39	40	97.50
Total (Producer)	178	97	35	30	16	5	7	6	54	31	41	500	
Producer Accuracy (%)	97.19	92.78	77.14	76.67	81.25	100.00	85.71	100.00	92.59	64.52	95.12		
Overall Accuracy:	**90.40**												
Kappa Coefficient:	**87.98**												

The accuracy assessment of the 1991 LULC confusion matrix indicates that the overall classification was highly accurate, with an overall accuracy of 90.40% and a Kappa coefficient of 87.98%, suggesting strong agreement beyond chance between the classified map and reference data. Crop land showed excellent performance with a user accuracy of 93.01% and a producer accuracy of 97.19%, indicating that most actual cropland pixels were correctly identified and very few non-cropland pixels were misclassified as crop land. Vegetation also performed well with high accuracies (user: 92.78%, producer: 92.78%), while marsh land, mangrove, salt marsh, and water body classes showed nearly

perfect producer accuracies in some cases, reflecting precise mapping of these specific land cover types. Barren land and tidal flat had relatively lower producer accuracies of 64.52% and 100% for tidal flat, indicating some misclassification with other classes like build-up areas and flooded flats. Similarly, built-up areas had minor confusion with barren land and some cropland, as indicated by non-zero off-diagonal values. Overall, the diagonal values in the matrix were dominant, showing that the majority of pixels were correctly classified, while the off-diagonal errors highlight areas where spectral similarities caused misclassifications. These accuracy measures provide a clear quantitative assessment of how well the 1991 LULC map represents actual land cover, helping identify the most reliable classes and those needing further refinement.

The 1991 LULC accuracy emphasizes the strengths and limitations of the classification approach. High accuracies for major classes like crop land, vegetation, and water body reflect effective use of training data, clear spectral separability, and successful cloud and shadow filtering. Misclassification among classes like barren land, built-up area, and tidal flat suggests that spectral similarities and transitional land covers can introduce errors, which is common in mixed or heterogeneous landscapes. The moderate user accuracy for flooded flat land (81.25%) and build-up areas (81.97%) indicates that some pixels assigned to these classes were incorrectly classified, potentially due to seasonal water presence or urban-rural transitions in 1991. These results highlight the importance of careful selection of training samples and the potential need for additional ancillary data to improve class discrimination. The Kappa coefficient of 87.98% reinforces that the overall agreement is strong but not perfect, emphasizing the role of intrinsic spectral overlaps in remote sensing data. This evaluation demonstrates that while the classification is generally reliable for analyzing large-scale LULC patterns, caution is needed when interpreting marginal or mixed land cover types. Future studies could enhance accuracy by incorporating higher-resolution imagery, multi-season composites, or field validation to reduce residual misclassifications and provide a more precise representation of the landscape in 1991.

The accuracy assessment of the 2001 LULC confusion matrix shows that the overall classification remained strong, with an overall accuracy of 89.60% and a Kappa coefficient of 87.00%, indicating substantial agreement between the classified map and reference data. Crop land again displayed high classification performance, with a user accuracy of 90.32% and a producer accuracy of 97.11%, reflecting effective identification of cropland pixels and minimal misclassification from other classes. Vegetation maintained high accuracy (user: 92.78%, producer: 88.24%), though the slight decline in producer accuracy compared to 1991 suggests minor confusion with other classes. Marsh land, mangrove, and water body classes showed perfect or near-perfect producer accuracies, reflecting reliable mapping of these distinct spectral classes. In contrast, classes like barren land, tidal flat, and flooded flat land had lower producer accuracies (66.67%, 100%, and 81.25% respectively), indicating some pixels were misclassified, likely due to mixed or transitional land cover types. The diagonal values of the matrix dominate, showing the majority of pixels were correctly classified, while off-diagonal values highlight areas where confusion occurred, such as minor misclassification between crop land and vegetation or built-up and barren areas. These results confirm that the classification was generally reliable across most land cover types while identifying specific classes that were more prone to error.

Table 3: Accuracy assessment of LULC 2001													
LULC class	Crop land	Vegetation	Shrub land	Marsh land	Flooded flat land	Mangrove	Salt marsh	Tidal flat	Buildup area	Barren land	Water body	Total (User)	User Accuracy (%)
Crop land	168	9	7	0	2	0	0	0	0	0	0	186	90.32
Vegetation	3	90	0	4	0	0	0	0	0	0	0	97	92.78
Shrub land	0	3	27	0	0	0	0	0	0	0	0	30	90.00
Marsh land	0	0	1	23	0	0	0	0	0	0	0	24	95.83
Flooded flat land	2	0	0	0	13	0	1	0	0	0	0	16	81.25
Mangrove	0	0	0	1	0	5	0	0	0	0	0	6	83.33
Salt marsh	0	0	0	1	0	0	6	0	0	0	0	7	85.71
Tidal flat	0	0	0	0	0	0	0	6	0		2	8	75.00
Buildup area	0	0	0	0	0	0	0	0	51	10	0	61	83.61
Barren land	0	0	0	0	1	0	0	0	4	20	0	25	80.00
Water body	0	0	0	1	0	0	0	0	0	0	39	40	97.50
Total (Producer)	173	102	35	30	16	5	7	6	55	30	41	500	
Producer Accuracy (%)	97.11	88.24	77.14	76.67	81.25	100.00	85.71	100.00	92.73	66.67	95.12		
Overall Accuracy:	**89.60**												
Kappa Coefficient:	**87.00**												

The 2001 LULC accuracy emphasizes both the strengths and limitations of the classification results. High accuracies for major classes like crop land, vegetation, and water body indicate that training samples, spectral separability, and preprocessing steps like cloud filtering were effective. The slight decrease in producer accuracy for vegetation and crop land compared to 1991 highlights potential challenges from changes in landscape patterns or seasonal differences affecting spectral signatures. Misclassification among built-up areas, barren land, and tidal flats indicates that spectral similarities and land cover heterogeneity contributed to classification errors, a common issue in remote sensing for complex landscapes. User accuracies above 80% for most classes indicate that the assigned

classifications are reasonably reliable, though some mixed pixels, particularly in marginal or transitional zones, reduce certainty. The Kappa coefficient of 87.00% confirms substantial agreement beyond chance but also signals that there is room for improvement. These results suggest that while the 2001 LULC map is suitable for analyzing broad land cover patterns and trends, caution is needed when interpreting minor or mixed classes. Future classifications could benefit from incorporating multi-seasonal imagery, higher-resolution data, or additional ancillary datasets to improve discrimination among spectrally similar land cover types and reduce residual errors in the classification. Overall, the accuracy assessment demonstrates a robust methodology capable of supporting land cover monitoring and change detection over time.

The 2011 LULC accuracy assessment reflects a highly reliable classification, with an overall accuracy of 90.00% and a Kappa coefficient of 87.48%, indicating strong agreement between the classified map and reference data. Crop land showed excellent classification performance with a user accuracy of 91.40% and producer accuracy of 96.05%, demonstrating that most cropland pixels were correctly identified and few non-cropland pixels were misclassified. Vegetation also maintained high accuracies at 92.78% for both user and producer measures, highlighting consistent mapping of vegetated areas over time. Marsh land, mangrove, and water body classes were also classified with very high reliability, reflected in producer accuracies above 95% for water bodies and perfect scores for mangrove and tidal flats. On the other hand, shrub land experienced a slight drop in producer accuracy to 69.44%, suggesting some misclassification into crop land or vegetation. Barren land and flooded flat land showed moderate accuracies, indicating minor errors, often due to spectral confusion with nearby built-up areas or transitional land cover types. The confusion matrix diagonal dominance shows that most pixels were classified correctly, while the off-diagonal cells highlight small areas of confusion among similar classes. User accuracies above 80% for most classes suggest that the assigned classifications are generally reliable for landscape analysis.

From a discussion perspective, the 2011 accuracy assessment demonstrates both the strengths and limitations of the classification. High accuracies for key classes like crop land, vegetation, and water body suggest effective selection of training samples, clear spectral differentiation, and proper preprocessing such as cloud masking and median composites. Misclassifications, particularly for shrub land and some built-up areas, indicate challenges in distinguishing classes with similar spectral reflectance or those located in heterogeneous landscapes. Moderate accuracies for barren and flooded flat lands reflect the difficulty in separating these classes from transitional or mixed pixels, a common issue in satellite-based LULC classification. The Kappa coefficient of 87.48% confirms substantial agreement beyond chance, reinforcing the robustness of the overall mapping approach. These results suggest that while the 2011 LULC map is suitable for broad-scale analysis of land cover patterns, caution should be exercised when interpreting classes prone to misclassification. Enhancing future classifications could involve multi-seasonal imagery, higher-resolution data, or integration of ancillary datasets such as soil, topography, or socio-economic information to improve spectral separability. Overall, the methodology demonstrates a solid and consistent approach to long-term LULC mapping, enabling the detection of temporal land cover changes with a reliable level of confidence.

Table 4: Accuracy assessment of LULC 2011													
LULC class	Crop land	Vegetation	Shrub land	Marsh land	Flooded flat land	Mangrove	Salt marsh	Tidal flat	Buildup area	Barren land	Water body	Total (User)	User Accuracy (%)
Crop land	170	4	10	0	2	0	0	0	0	0	0	186	91.40
Vegetation	3	90	0	4	0	0	0	0	0	0	0	97	92.78
Shrub land	2	3	25	0	0	0	0	0	0	0	0	30	83.33
Marsh land	0	0	1	23	0	0	0	0	0	0	0	24	95.83
Flooded flat land	2	0	0	0	13	0	1	0	0	0	0	16	81.25
Mangrove	0	0	0	1	0	5	0	0	0	0	0	6	83.33
Salt marsh	0	0	0	1	0	0	6	0	0	0	0	7	85.71
Tidal flat	0	0	0	0	0	0	0	6	0		2	8	75.00
Buildup area	0	0	0	0	0	0	0	0	53	8	0	61	86.89
Barren land	0	0	0	0	1	0	0	0	4	20	0	25	80.00
Water body	0	0	0	1	0	0	0	0	0	0	39	40	97.50
Total (Producer)	177	97	36	30	16	5	7	6	57	28	41	500	
Producer Accuracy (%)	96.05	92.78	69.44	76.67	81.25	100.00	85.71	100.00	92.98	71.43	95.12		
Overall Accuracy:	**90.00**												
Kappa Coefficient:	**87.48**												

Table 5: Accuracy assessment of LULC 2021													
LULC class	Crop land	Vegetation	Shrub land	Marsh land	Flooded flat land	Mangrove	Salt marsh	Tidal flat	Buildup area	Barren land	Water body	Total (User)	User Accuracy (%)
Crop land	173	4	7	0	2	0	0	0	0	0	0	186	93.01
Vegetation	3	90	0	4	0	0	0	0	0	0	0	97	92.78

Shrub land	0	3	27	0	0	0	0	0	0	0	0	30	90.00
Marsh land	0	0	1	23	0	0	0	0	0	0	0	24	95.83
Flooded flat land	2	0	0	0	13	0	1	0	0	0	0	16	81.25
Mangrove	0	0	0	1	0	5	0	0	0	0	0	6	83.33
Salt marsh	0	0	0	1	0	0	6	0	0	0	0	7	85.71
Tidal flat	0	0	0	0	0	0	0	6	0		2	8	75.00
Buildup area	0	0	0	0	0	0	0	0	50	11	0	61	81.97
Barren land	0	0	0	0	1	0	0	0	4	20	0	25	80.00
Water body	0	0	0	1	0	0	0	0	0	0	39	40	97.50
Total (Producer)	178	97	35	30	16	5	7	6	54	31	41	500	
Producer Accuracy (%)	97.19	92.78	77.14	76.67	81.25	100.00	85.71	100.00	92.59	64.52	95.12		
Overall Accuracy:	**90.40**												
Kappa Coefficient:	**87.98**												

The 2021 LULC accuracy assessment indicates a highly reliable classification, with an overall accuracy of 90.40% and a Kappa coefficient of 87.98%, reflecting strong agreement between the classified map and reference data. Crop land remained the most accurately classified class, with a user accuracy of 93.01% and a producer accuracy of 97.19%, suggesting that most cropland areas were correctly identified and very few non-crop areas were misclassified. Vegetation also showed high reliability, with both user and producer accuracies at 92.78%, highlighting consistent mapping over the study area. Water body, mangrove, and tidal flat classes achieved perfect or near-perfect producer accuracies, demonstrating that distinct spectral characteristics made these classes easier to distinguish. Shrub land had a moderate producer accuracy of 77.14%, indicating some misclassification with crop land or vegetation, while barren land had the lowest producer accuracy of 64.52%, reflecting challenges in distinguishing it from adjacent built-up areas or transitional landscapes. Built-up areas had minor misclassification, mostly with barren land and some cropland. Off-diagonal values in the confusion matrix reveal these specific misclassifications, while the dominant diagonal values confirm that the majority of pixels were correctly classified. Flooded flat land, salt marsh, and marsh land also showed moderate to high accuracies, indicating overall robustness in the mapping of diverse land cover types.

From a discussion standpoint, the 2021 LULC results underscore the effectiveness and consistency of the classification methodology over time. The high accuracies for major land cover classes such as crop land, vegetation, and water bodies suggest that careful selection of training samples, cloud-free composites, and spectral separability contributed to reliable classification. Some misclassification, particularly among shrub land, barren land, and built-up areas, points to challenges in discriminating spectrally similar or mixed pixels, which is common in heterogeneous landscapes. The Kappa coefficient of 87.98% reinforces that the overall map agreement is strong beyond random chance, supporting its use for long-term land cover analysis. User accuracies above 80% for most classes indicate that the mapped classes can be interpreted with confidence, though caution is advised for transitional or ambiguous areas. These findings suggest that the 2021 LULC map provides a solid foundation for evaluating trends in urban expansion, vegetation dynamics, and wetland changes. Further refinement could involve multi-season imagery, higher-resolution satellite data, or ancillary geographic information to reduce residual misclassifications. Overall, the methodology demonstrates consistent, reliable performance across decades, making it suitable for environmental monitoring, land management planning, and detecting long-term landscape changes.

3.2 NDBI:

In 1991, NDBI map shows clearly that the non built up areas prevail and dominate the landscape, which depicts a largely rural and agrarian environment. Occupying extremely low spatial scale and being dispersed in separated locations, built up areas do not create continuous clusters. These accumulated patches are mostly located along the eastern coastline and riverine valleys implying the existence of small settlements, port activities and early urban centres. When compared to both area and percentage, the built up land comprises of a small proportion of the total geographical cover with over ninety five percent of the area not being built up. This is in the spatial pattern that shows low population pressure and the minimal development of infrastructure in this period. The cities are characterised by an excessive urbanization, which is not accompanied by extension. In general, the NDBI scenario in 1991 can be seen as a primitive form of urbanization with little natural and agricultural landscapes being transformed.

In 2001, one can observe a slow rise in built up area as compared to the year 1991. Though the share of the total area occupied by non built up land remains enormous, the spatial extent of the built up surfaces and percentages are experiencing a visible increase. Growth is more evident in the eastern side of the area under study as the clusters of buildings seem more compact and intact. Little linear expansions along the transportation paths and bank sides are also beginning to appear, denoting the power of connectivity and economic activities. Still, the percentage of built up land is a small portion of total area, however growth rate is higher than that of last decade. This stage is the point of space consolidation of settlements. The trend in 2001 indicates an early urbanization as a result of population increase and better accessibility.

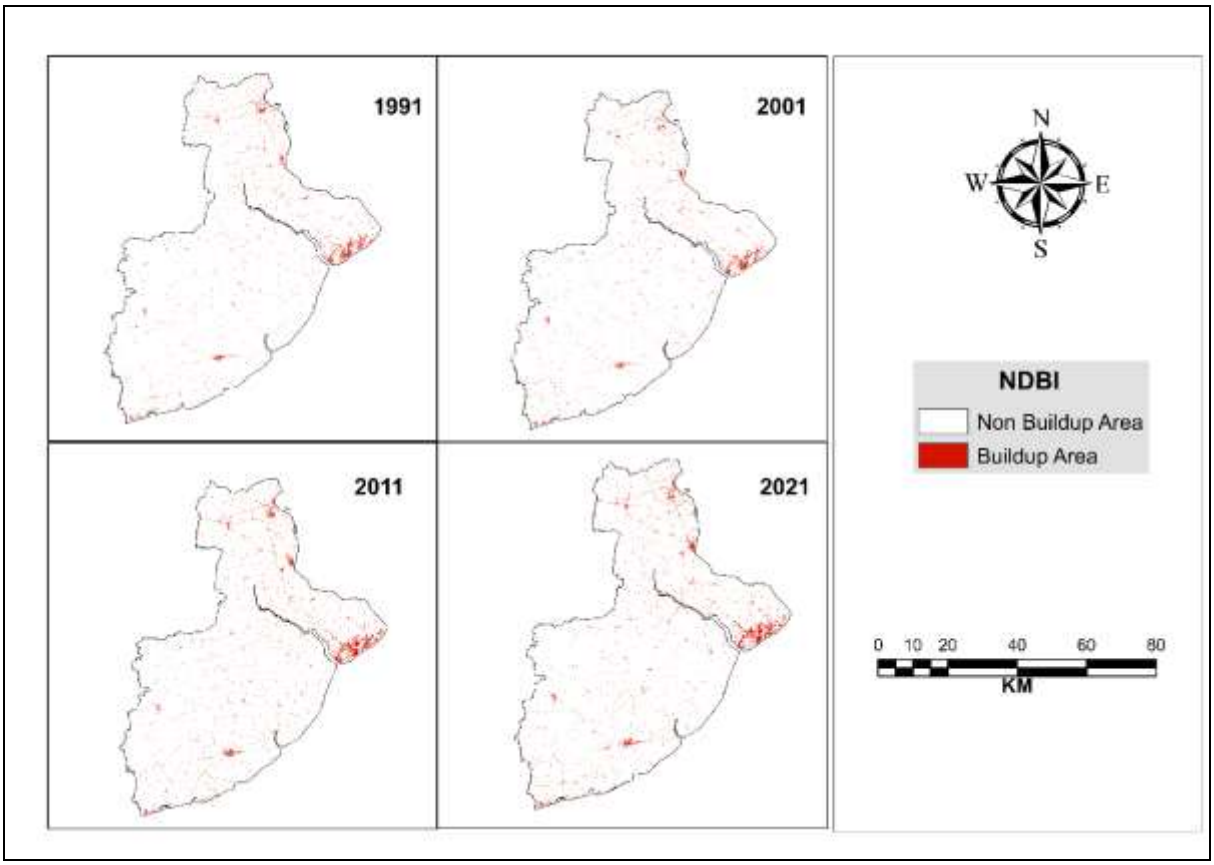

Figure 3: Spatiotemporal distribution of built-up and non-built-up areas in Purba Medinipur district derived from NDBI for 1991, 2001, 2011 and 2021.

The NDBI map shows that there is a more intense growth of built-up areas throughout the region in 2011. The overall size of the area covered by the built-up land grows even more and its percentage ratio to the landscape is even greater than in previous years. The intensity of built-up clusters is evident in the eastern coastal area and the emergence of new clusters in the central and northern areas of the area of study. The spatial distribution implies the horizontal extension of the already existing settlements as well as the development of new centers of growth. Even though the non built up areas are still on the lead in the total percentage share, the percentage share decreases gradually. This decade is more predominant in infrastructure development and urban sprawl. The situation in 2011 is about the shift towards a more structured and integrated urban development as opposed to the dispersed settlement (Figure 3).

The spatial extent and percentage of the built up area is the greatest in 2021 compared to all the years that have been seen. The urbanized land is increasing significantly into massive and continuous clusters, particularly in the eastern side and transport corridors. The lent area of built up land grows significantly and in turn, the ratio of non built up land decreases accordingly. Though non built up area continues to occupy most part of the area, the portion of built up land now constitutes a distinct part of the landscape. The growth trend is an indication of increased urbanization, concentration of population, and infrastructural expansion. Urban sprawl can be observed through the peripheral growth of the already existing urban centers. The map of 2021 emphasizes the compound effect of thirty years of pressure development (Figure 3).

In general, the temporal trend of NDBI since 1991-2021 shows the presence of a steady upward trend in built up area in terms of spatial coverage and proportion of the total area. The scenery changes to a more

intricate mosaic that is more urban footprints as compared to the mostly non built up rural landscape. The early decades were characterized by patchy and sparse built-up areas whereas the recent years were characterized by the consolidation and protrusion of the settlements. The growing built up percentage reflects the growing anthropogenic pressure and change of land surfaces. This protracted trend represents the increasing impact of urbanization on land use processes and the importance of sustainable planning that will control the future development and preserve the non built up lands around.

3.3 NDVI:

The NDVI distribution of 1991 shows that the moderate vegetation condition was a major part of the landscape with the area measuring approximately 32,336.64 km 2 which represents almost 76.26 percent of the area. This implies that the major portion of the area was favourable to stable agricultural produce and mixed vegetation with fair levels of greenness. The well-vegetated zoned areas with healthy biomass occupy approximately 8,266.73 km 2 or 19.49 percent which could be linked to irrigated crop lands and patches of natural vegetation. The very high NDVI coverage is also restricted to 802.73 km 2, which is 1.89 percent, meaning that these areas are either deeply vegetated like forest patches or extremely productive crop-producing areas. The size of low NDVI areas is 651.66 km 2 or 1.54 percent, whereas the size of very low NDVI areas is only 347.72 km 2 or 0.82 percent, which is mostly built-up areas, bare soil, water or stressed vegetation. The NDVI pattern of 1991 shows in general that the topography is majorly vegetated and productive with minimal degraded or non-vegetated areas (Figure 4).

The change in the NDVI structure can be noticed by the year 2001, with moderate vegetation still consisting of the bulk. The moderate NDVI category grows considerably to 34,788.40 km 2 which corresponds to 82.04 percentage of the total area, which showed overall expanded moderately vegetated areas. The high NDVI values plummet to 5345.01 km 2 or 12.60 percent, implying that there is a decrease in the dense vegetation cover. NDVIs are also incredibly high and tend to reduced slightly to 744.94 km 2 or 1.76 percent, which represents the sustained pressure on highly productive vegetation. There is an increase in low NDVI areas to 1,135.39 km 2 or 2.68 percent and very low NDVI areas to 391.51 km 2 or 0.92 percent indicating slow growth of developed land or vegetation stress. These transformations suggest that the vegetation has become less dense and more moderate, perhaps because of agricultural intensification and land use (Figure 4).

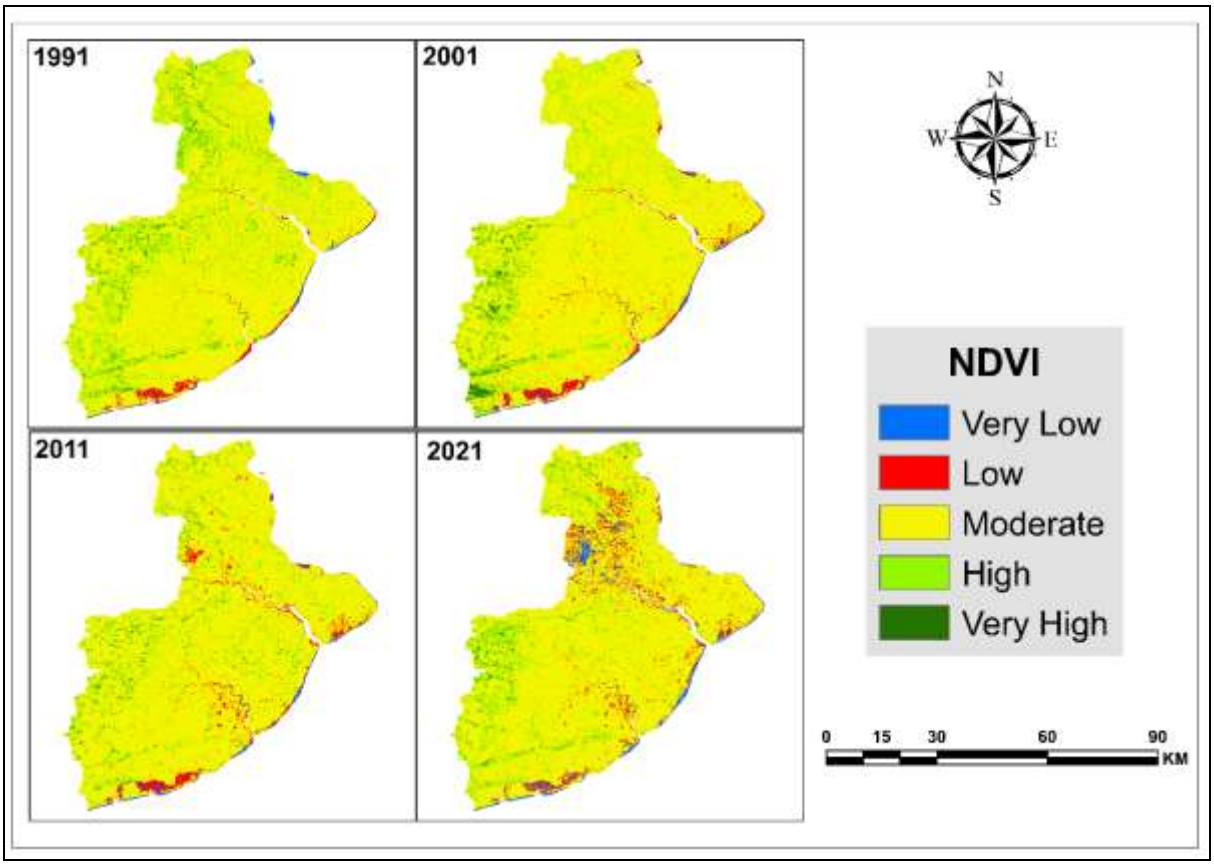

Figure 4: Spatiotemporal distribution of NDVI classes (very low to very high vegetation cover) in Purba Medinipur district for 1991, 2001, 2011 and 2021.

The NDVI distribution of 2011 further supports the fact that there is preponderance of moderate vegetation conditions in the region. The moderate class of NDVI value grows up to 35,359.05 km 2 or 83.38 percent of the total area, pointing to a uniform but extensive vegetation cover. The region of high NDVI remains decreasing to 4,560.32 km 2 or 10.75 percent indicating additional deterioration of thick vegetation beds. Very high NDVI is reduced to 681.74 km 2 or 1.61 percent, which supports the tendency of the reduction of highly productive vegetation. Low NDVI areas are increasing up to 1,433.88 km 2 or 3.38 percent, and very low NDVI areas are approximately 370.49 km 2 or 0.87 percent. The rising intensity of low NDVI areas indicates the rising anthropogenic stress, land degradation, or seasonal vegetation stress. On balance, the situation of 2011 is characterized by slow homogenization of vegetation state with less sharp extremes of high greenness (Table 2).

Table 6: Spatiotemporal Distribution of NDVI Classes in Purba Medinipur District (1991–2021) showing Area and Percentage (%)

Class	1991		2001		2011		2021	
	Area	% of Area	Area	% of Area	Area	% of Area	Area	% of Area
Very Low	347.72	0.82	391.51	0.92	370.49	0.87	994.83	2.35
Low	651.66	1.54	1135.39	2.68	1433.88	3.38	1828.01	4.31
Moderate	32336.64	76.26	34788.40	82.04	35359.05	83.38	37459.33	88.34

High	8266.73	19.49	5345.01	12.60	4560.32	10.75	1535.52	3.62
Very High	802.73	1.89	744.94	1.76	681.74	1.61	587.79	1.39

The NDVI distribution is the strongest change that has occurred during the period of study (2021). The moderate areas of NDVI increase enormously to 37,459.33 km 2, which occupies approximately 88.34 percent of the overall area, and is overtaken by moderately vegetated or cultivated land. Conversely, the high NDVI regions reduce significantly to 1,535.52 km 2 or 3.62 percent indicating considerable reduction of high vegetations. Very high NDVI also goes down to 587.79 km 2 or 1.39 percent implying that there is not much natural vegetation left which is healthy. Low NDVI areas grow substantially to 1,828.01 km 2 or 4.31 percent, very low NDVI areas grow drastically to 994.83 km 2 or 2.35 percent, signifying the growth in built up land, barren or grossly strained vegetation. This tendency demonstrates the expanding human activity and environmental pressure in the area (Table 2).

In general, the time NDVI analysis of 1991-2021 proves the obvious change in the state of vegetation and landscape well-being. Although moderate NDVI remains dominant and grows with time, the high and very high classes of NDVI exhibit a stable decrease, which suggests disappearance of dense and healthy vegetation cover. At the same time, there is a steady rise in low and very low NDVI classes, which is the answer to growing urbanization, land degradation, and the exposure of the surface. The transition proposes a shift to less resilient vegetation structure that is more uniform. All these trends lead to the conclusion that there is an escalating anthropogenic stress and varying land management systems that have affected the vegetation dynamics in the past three decades.

3.4 LST:

The LST map of 1991 reveals an extremely dissimilar thermal terrain where there exists a distinct difference between cooler and warmer areas in the region. The lower LST values of about 17.86˚C are only found in places that may be characterized by dense vegetation cover, water bodies, and comparatively untouched surfaces and as such, the evapotranspiration and moisture availability are higher. Conversely, the higher LST values of up to 37.63˚ C are confined primarily to the southern and peripheral areas, either indicating a bare surface or sparse vegetation or limited land use intensification. According to the spatial pattern, it can be stated that natural land cover was still a major factor in controlling surface temperature at this time. It is also evidenced by the patchy distribution of warm and cool zones and limited urban or infrastructural development and more dominance by geomorphology and hydrology. On the whole, the situation in 1991 is a relatively equal thermal environment with moderate extremes and high local diversity.

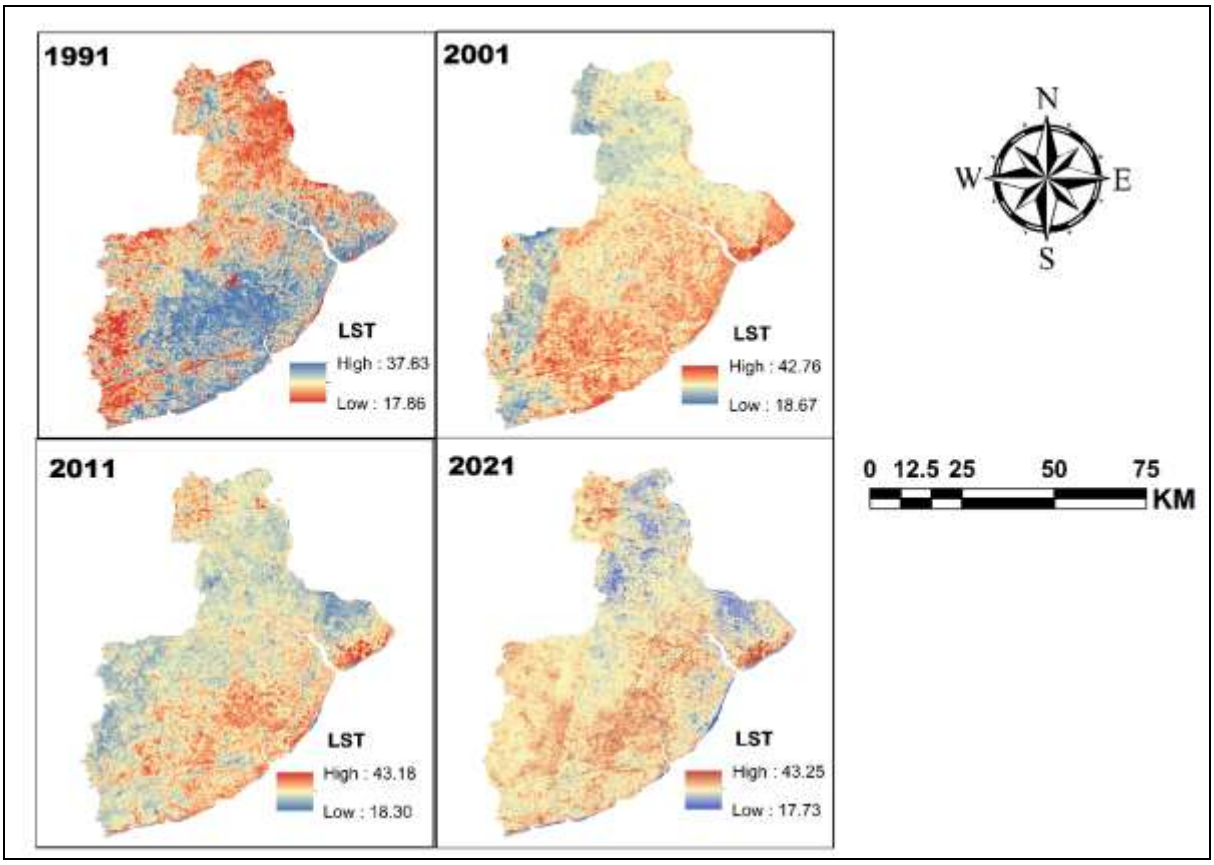

Figure 4: Spatio-temporal distribution of LST in Purba Medinipur District (1991-2021)

As of 2001, the LST pattern displays an evident rise in total surface temperature as well as a decrease in cooler areas. The peak LST increases abruptly at approximately 42.76˚C, which signifies the increase in the intensity of the surface heating processes. Warmer regions are more spatially continuous, especially in the central and southern regions of the region and would indicate expansion of built up land agricultural intensification or vegetation degradation. There have been cooler regions with lowest LST of 18.67˚C that are now more fragmented and restricted, perhaps only along river corridors forest patches or irrigated lands. Such change connotes the diminishing moisture content of the surface as well as a decrease in thermal control capacity of the landscape. The move to a patch dominated pattern to a more homogeneous warm surface reflects the growing anthropogenic impact. The 2001 map is thereby an important stage of thermal change due to land cover change (Figure 4).

The LST distribution of 2011 perpetuates this pattern of warming but it also demonstrates a more complicated distribution on a spatial basis. The maximum LST is about 43.18 o C, and the minimum is quite consistent at about 18.30˚C. The southern and eastern regions exhibit large areas of high temperature zones, which means that there is heat stress on the areas. Nevertheless, there is evidence of reappearance or remnants of cooler conditions in the north and central areas indicating the localized effect of mitigation likely through vegetation regrowth irrigation methods or topography. Although moderately high and high LST values were dominant in these localized cool zones, cumulative effects of land use change and climatic variability were likely contributors to the overall dominance of moderately high and high LST values. The difference between hot and cold regions are enhanced and it suggests that there are more thermal gradients. The time is a transitional phase whereby there is a wide prevalence of warming but spatial controls can still be observed (Figure 4).

The map of LST in 2021 shows more consolidated and intense thermal regime in the whole region. The upper LST marginally rises to approximately 43.25°C and the lower temperature decreases slightly to 17.73°C signifying improved thermal extremes. The high temperature areas cover the larger part of the landscape, particularly in the central southern and eastern areas which points to vast surface alteration and diminished vegetation buffering. However, cooler regions are now confined and linear, and are often along river routes or certain areas of land cover, and represent restricted cooling processes. The homogeneity of high LST values in space is indicative of persistent urbanization agricultural stress and long run land cover change. The 2021 pattern shows that there is a mature stage of thermal intensification as compared to previous years. On the whole, the historical development of 1991 to 2021 evidently shows a steady rise in the surface temperature and a drop in natural thermal control of the area.

3.5 Discussion

The land use change and vegetation dynamics interaction is even greater in the year 2011, and it has a significant impact on the distribution of LST. According to LULC statistics as well as NDBI maps, the decrease in cropland area is minor and the growth in built up land is quite high. The NDVI analysis indicates that high and very high vegetation classes continue to decrease, and the low NDVI areas continue to expand(Dapke et al., 2025). This means reduction in the vegetation, change to settlements and exposure to the surface. Displacement of marsh land, tidal flats and mangrove submergence contributes further to natural cooling processes. These intertwined modifications increase the sensible heat flux and decrease the latent heat flux resulting into an increase in land surface temperatures. LST maps indicate greater spatial continuity of warmer regions, particularly around urbanizing and coastal regions. The situation in 2011 is a distinct shift towards thermal stress that is anthropogenically induced (Khan et al., 2023).

The developments that took place in the land surface temperature in 1991 can be greatly attributed to the prevalence of cropland and moderate to high NDVI conditions within the area. In the time, there was over ninety three percent of agricultural lands and NDVI analysis revealed widespread moderate and high vegetation greenness. This kind of land cover tends to favour evapotranspiration, soil moisture storage and shading which aids in the regulation of surface temperature. The built up areas were small and sparse as indicated by the very low values of NDBI and as well as the low extent of built-up areas minimized the existence of heat trapping impervious surfaces (Mondal et al., 2021). There were also wetlands, tidal flats, marsh land and water bodies although not much in area that added to local cooling. Consequently, the LST values in 1991 were on a reasonable level with high spatial heterogeneity. The topography remained mostly natural and agricultural, such that the ecological process efficiently compensated high and low temperatures (Haldar et al., 2023).

By 2001, there are minor yet significant changes to the patterns of LULC, NDVI and NDBI that start to affect the LST. In spite of the fact that the area of croplands is still dominant, there are minor declines in the vegetation cover and wetlands classes, as well as the premature growth of built up areas. The results of NDVI show that the proportion of high and very high vegetation classes changed into moderate degrees of greenness that may imply the expansion of agriculture and potential stress created by natural vegetation. The changes decrease the efficiency of evapotranspiration, and they enlarge the surfaces of soil, which are exposed to heat. The NDBI maps demonstrate gradual concentration of the built up areas around the coastal areas and transport corridors, which introduce impervious materials that absorb and trap heat. As a result, the value of LST increases significantly as compared to 1991, particularly where

land transformation is taking place. The 2001 era therefore indicates the inception of the Anthropogenic thermal changes to the terrain (Nautiyal et al., 2025; Pandey et al., 2023; Tiwari et al., 2025).

Implementation of LST transformations is closely associated with land cover change that is cumulative and increased human activity as of 2021. The area covered by crops reduces significantly, whereas the area occupied by built-up areas and water bodies grows significantly, which also signifies significant changes in land and hydrological regimes (N et al., 2025). The NDVI results indicate a preponderance of moderate vegetation and extreme declines in the high and very high NDVI classes and a fast increase in low and very low NDVI areas. This implies extensive vegetation stress, urban growth and surface alteration. The NDBI maps verify the presence of thick and continuous built up clusters, which are heat islands since they have a high thermal inertia and low moisture content. Increased water bodies may have a local but a net negative impact by conversion of large areas of land, even though it can be seen to reduce the temperature. As a result, LST will achieve its peak values and become more spatially homogeneous. The 2021 trend indicates an adult phase of human-induced warming on the local level (Kumari et al., 2018).

The recorded degradation in value of NDVI between high and very high classes over time is closely related to the alteration in LULC and NDBI. Dense vegetation and healthy cropland in previous years ensured ecological balance because of higher values of NDVI. Density and continuity of vegetation is reduced with growth of built up areas, agricultural intensification and land degradation with time. Moderate NDVI dominance represents vegetation that is not as strong as it can be, and most commonly it is monocropped or stressed. Low and very low NDVI expansion indicates bare soil, settlements, roads and poor land. It is a vegetation degradation that has a direct effect on the surface energy balance by slowing evapotranspiration. Consequently, NDVI patterns are a good explanation of the increase in LST patterns over decades (Vanlalchhuanga et al., 2025).

It is shown that urban growth as determined using NDBI is very critical in increasing both LST and decreasing NDVI. Concrete, asphalt, and rooftops are built up surfaces that trap solar radiations during the day and slow down the radiations of heat at night. The increasing thermal impact of built up area is more and more evident as the areas increase in 1991 as separate oases to the current 2021 oases of dense cluster formation. Urban sprawl tends to cover croplands, wetlands and vegetation, resulting in the concomitant decrease in NDVI and the subsequent increase in LST. Green spaces are also further divided by linear growth along roads and riverbanks. The net effect is that localized heat islands and eventually regional heat islands are created. Hence, NDBI trends are very powerful in elucidating the spatial concentration of high LST zones (Pandey et al., 2024).

Wetland and coastal land cover changes also play a big part in the observed changes in LST and NDVI. Marsh land, tidal flats, and mangroves are in decline since 1991 to 2021 with exception of slight recovery in the latter years. Such ecosystems are very efficient in temperature regulation in terms of moisture retention and shading. Loss of them decreases the ability of the landscape to regulate heat particularly in the coastal and low lands. The NDVI values in these areas also reduce when salinity intrusion and land encroachment is on the rise. The loss of such natural buffers increases the surface heating and leads to the increase of LST in the locality. The pressure of coastal development is therefore an indirect but significant contributor in thermal change (Santhosh & Shilpa, 2023).

Another important source of LULC, NDVI, LST dynamics connection is agricultural intensification. The cropland although it is mainly dominant during the period of study, its internal characteristics vary greatly. The intensive monocropping and mechanized farming systems are slowly replacing traditional

mixed cropping systems. These practices decrease the diversity of crops, soil water retention, and seasonal vegetation cover and reduce the NDVI values. Bare soil that is present in harvested or fallow fields warms quickly and raises LST. Localized irrigation can partly cool the climate, but no longer has the capacity to compensate the massive conversion of land. Thus, high cropland percentage still does not lead to the decrease of the LST because of qualitative land management changes (Santhosh & Shilpa, 2023).

The trends of NDVI and LST are also affected by hydrological changes in the form of increase in water body area in 2021. Increase in water bodies can either be through flooding, aquaculture, widening of rivers or change in rainfall under climatic influence. Although water surfaces may cool locally, their abrupt expansion is a characteristic of environmental stress, e.g., flooding or subsidence of the land. There can be vegetation loss, soil erosion and land abandonment around the areas resulting into the reduction of NDVI values. In addition, stagnant waters or shallow water bodies may at times enhance humidity and the night temperature. Therefore, hydrological changes have a non-uniform effect on LST(Bala et al., 2024).

The background driver that is likely to increase land cover induced changes is climate variability. Increased temperatures in the region, changed precipitation patterns, and the occurrence of extreme events, aggravate vegetation stress and land degradation. These climatic conditions give rise to the effects of urbanization and conversion of land that are recorded by NDVI and NDBI patterns. Although the land use change might be limited in different areas, increased LST may be witnessed because of extended climatic warming. Thus, the increases in LST that are observed can never be due to a change in land cover alone but are due to the summation of land atmosphere interactions (Guha & Govil, 2021; Malik et al., 2019).

Much of the changes in the LULC, NDVI, and NDBI are based on socioeconomic development over a period of thirty years. Land conversion and settlement growth are caused by population growth, infrastructure growth, industrial growth and economic diversification. These processes transform the surface features, decrease the green cover, and augment non-porous areas. This trajectory of development is manifested in the spatial coincidence of the high NDBI and high LST areas. Meanwhile, there is a gradual loss of natural ecosystems due to low conservation efforts. Multi index changes can thus be explained as a result of socio economic pressure (Das et al., 2021; Gupta et al., 2023; Shahfahad et al., 2020).

In general, the dynamics of LST, NDVI, NDBI, and LULC over the years show a closely interconnected pattern of environmental change. Low built up extent, moderate surface temperatures, high greenness of vegetation and early decades are agrarian dominated. As time progresses, the growing urbanization, vegetation stress, wetlands loss, and land management alteration induce the NDVI deterioration and NDBI growth. These alterations have a direct effect on surface energy balance, and they cause steady LST increase. The compound analysis recognizes that land use choices and human practices transform thermal and ecological conditions over a landscape (Roy & Kasemi, 2021; Sinha et al., 2011; Sreenivasulu & Udaya Bhaskar, 2010).

4.0 Conclusion:

The study provides a comprehensive spatiotemporal assessment of land use land cover transformation and its influence on surface thermal and ecological conditions in Purba Medinipur district during 1991–2021 using Landsat based remote sensing and GIS techniques. Multi decadal mapping of LST, NDVI,

NDBI, and LULC clearly demonstrates that the study area has experienced continuous landscape modification, dominated by declining cropland share, increasing built up expansion, and significant alteration of wetland and water body classes. The vegetation condition analysis indicates a gradual shift from high and very high NDVI zones toward moderate and low NDVI categories, reflecting increasing vegetation stress and fragmentation. Simultaneously, the increasing NDBI values and spatial clustering of built-up areas highlight rapid urbanization and infrastructure growth, which correspond strongly with intensified surface warming patterns in the LST maps. Overall, the results confirm that anthropogenic land transformation has been a major driver of thermal stress and ecological change in this coastal agrarian district. The integrated use of multiple indices and quantitative area-based statistics strengthens the understanding of interlinkages among land cover conversion, vegetation dynamics, built up growth, and surface temperature variability, providing a strong scientific basis for environmental management and climate adaptation planning.

Despite the robustness of the multi-index approach, the study has certain limitations that should be acknowledged. The Landsat based analysis, though consistent and reliable, is constrained by 30 m spatial resolution, which may not fully capture small scale settlements, narrow coastal features, and fragmented vegetation patches. The annual mean composites may also smooth seasonal variability, potentially masking short-term extremes such as peak summer heating or cyclone induced vegetation loss. In addition, the LULC classification accuracy depends on the quality and representativeness of training samples, and some confusion between spectrally similar classes such as barren land and built-up land is possible.

Future research should incorporate higher resolution satellite data such as Sentinel 2 or commercial imagery, and include seasonal LST NDVI analysis to better capture intra annual dynamics. The integration of ground based meteorological observations, soil moisture information, and socioeconomic drivers would further enhance causal interpretation of changes. Moreover, advanced machine learning classifiers and change detection models could improve mapping precision and provide more detailed insight into transformation pathways. Such future efforts will strengthen monitoring of climate vulnerability, support sustainable land use planning, and assist in designing ecosystem-based adaptation strategies for coastal districts like Purba Medinipur.

Reference:

1. Acharya, S., Hori, T., & Karki, S. (2023). Assessing the spatio-temporal impact of landuse landcoverchange on water yield dynamics of rapidly urbanizing Kathmandu valley watershed of Nepal. Journal of Hydrology: Regional Studies, 50. https://doi.org/10.1016/j.ejrh.2023.101562
2. Ashwini, K., & Sil, B. S. (2022). Impacts of Land Use and Land Cover Changes on Land Surface Temperature over Cachar Region, Northeast India—A Case Study. Sustainability (Switzerland), 14(21). https://doi.org/10.3390/su142114087
3. Bala, R., Pratap Yadav, V., Nagesh Kumar, D., & Prasad, R. (2024). Exploring the relationship of land surface parameters and air pollutants with land surface temperature in different cities using satellite data. Advances in Space Research, 74(7). https://doi.org/10.1016/j.asr.2024.06.031
4. Chakraborty, S., John, B., Das, S., & Maity, P. K. (2020). Examining the extent of seawater intrusion from groundwater quality analysis at Purba Medinipur coast of India. Journal of the Indian Chemical Society, 97(4).

5. Dapke, P. P., Nagare, S. M., Quadri, S. A., Bandal, S. B., Gaikwad, R. M., & Baheti, M. R. (2025). Seasonal Analysis of Vegetation, Moisture, Urbanization, and Land Surface Temperature (LST) Using NDVI, NDMI, NDWI, and NDBI Indices: A Case Study of Sillod, Maharashtra. IEEE International Conference on "Computational, Communication and Information Technology", ICCCIT 2025. https://doi.org/10.1109/ICCCIT62592.2025.10928110
6. Das, N., Mondal, P., Sutradhar, S., & Ghosh, R. (2021). Assessment of variation of land use/land cover and its impact on land surface temperature of Asansol subdivision. Egyptian Journal of Remote Sensing and Space Science, 24(1). https://doi.org/10.1016/j.ejrs.2020.05.001
7. Dolui, S., & Sarkar, S. (2024). Modelling landuse dynamics of ecologically sensitive peri-urban space by incorporating an ANN cellular automata-Markov model for Siliguri urban agglomeration, India. Modeling Earth Systems and Environment, 10(1). https://doi.org/10.1007/s40808-023-01771-w
8. Gayen, S., Villalta, I. V., & Haque, S. M. (2020). Comparative social vulnerability assessment in Purba Medinipur district, West Bengal, India. European Journal of Geography, 11(1). https://doi.org/10.48088/ejg.s.gay.11.1.93.107
9. Gayen, S., Villalta, I. V., & Haque, S. M. (2022). Flood Risk Assessment and Its Mapping in Purba Medinipur District, West Bengal, India. Water (Switzerland), 14(7). https://doi.org/10.3390/w14071049
10. Govil, H., Guha, S., Dey, A., & Gill, N. (2019). Seasonal evaluation of downscaled land surface temperature: A case study in a humid tropical city. Heliyon, 5(6). https://doi.org/10.1016/j.heliyon.2019.e01923
11. Guha, S., & Govil, H. (2021). A long-term monthly analytical study on the relationship of LST with normalized difference spectral indices. European Journal of Remote Sensing, 54(1). https://doi.org/10.1080/22797254.2021.1965496
12. Gupta, R., Sharma, M., Singh, G., & Joshi, R. K. (2023). Characterizing urban growth and land surface temperature in the western himalayan cities of India using remote sensing and spatial metrics. Frontiers in Environmental Science, 11. https://doi.org/10.3389/fenvs.2023.1122935
13. Haldar, S., Mandal, S., Bhattacharya, S., & Paul, S. (2023). Dynamicity of land use/land cover (LULC): An analysis from peri-urban and rural neighbourhoods of Durgapur Municipal Corporation (DMC) in India. Regional Sustainability, 4(2). https://doi.org/10.1016/j.regsus.2023.05.001
14. Juhadi, Sanjoto, T. B., Pratiwi, E. S., Trihatmoko, E., Istiqomah, & Findayani, A. (2021). Rural-Urban Transformation and Landuse Dynamics in Gunungpati on the Northern Flank of Mt. Ungaran, Semarang, Indonesia. Indonesian Journal of Geography, 53(2). https://doi.org/10.22146/ijg.52385
15. Keerthi Naidu, B. N., & Chundeli, F. A. (2023). Assessing LULC changes and LST through NDVI and NDBI spatial indicators: a case of Bengaluru, India. GeoJournal, 88(4). https://doi.org/10.1007/s10708-023-10862-1
16. Khan, R., Aribam, B., & Alam, W. (2023). Estimation of impacts of land use and land cover (LULC) changes on land surface temperature (LST) within greater Imphal urban area using geospatial technique. Acta Geophysica, 71(6). https://doi.org/10.1007/s11600-023-01159-5
17. Kumar, S., & Singh, R. (2025). Geospatial approach to analyse the impact of urban development on the urban heat island in Hisar city, Western Haryana, India. Theoretical and Applied Climatology, 156(2). https://doi.org/10.1007/s00704-025-05366-6

18. Kumari, B., Tayyab, M., Shahfahad, Salman, Mallick, J., Khan, M. F., & Rahman, A. (2018). Satellite-Driven Land Surface Temperature (LST) Using Landsat 5, 7 (TM/ETM+ SLC) and Landsat 8 (OLI/TIRS) Data and Its Association with Built-Up and Green Cover Over Urban Delhi, India. Remote Sensing in Earth Systems Sciences, 1(3–4). https://doi.org/10.1007/s41976-018-0004-2
19. Malik, M. S., Shukla, J. P., & Mishra, S. (2019). Relationship of LST, NDBI and NDVI using landsat-8 data in Kandaihimmat watershed, Hoshangabad, India. Indian Journal of Geo-Marine Sciences, 48(1).
20. Martinez, A. de la I., & Labib, S. M. (2023). Demystifying normalized difference vegetation index (NDVI) for greenness exposure assessments and policy interventions in urban greening. Environmental Research, 220. https://doi.org/10.1016/j.envres.2022.115155
21. Mondal, A., Guha, S., & Kundu, S. (2021). Dynamic status of land surface temperature and spectral indices in Imphal city, India from 1991 to 2021. Geomatics, Natural Hazards and Risk, 12(1). https://doi.org/10.1080/19475705.2021.2008023
22. Mukherjee, F. (2022). Environmental Impacts of Urban Sprawl in Surat, Gujarat: An Examination Using Landsat Data. Journal of the Indian Society of Remote Sensing, 50(6). https://doi.org/10.1007/s12524-022-01509-8
23. N, S., M, R., S, N., & L, P. (2025). Correlation Between LST, NDVI and NDBI with Reference to Bengaluru Urban, Karnataka. International Journal For Multidisciplinary Research, 7(4). https://doi.org/10.36948/ijfmr.2025.v07i04.48420
24. Nautiyal, A., Juneja, G., & Singh, S. P. (2025). Spatial Analysis and Forecasting of Land Use Dynamics Using NDVI, NDBI, LST, and LULC: A Case Study of Srinagar Garhwal, India. Land Degradation and Development. https://doi.org/10.1002/ldr.70302
25. Pandey, A., Mondal, A., & Guha, S. (2024). Assess the relationship of land surface temperature with nine land surface indices in a northeast Indian city using summer and winter Landsat 8 data. Cogent Engineering, 11(1). https://doi.org/10.1080/23311916.2024.2382885
26. Pandey, A., Mondal, A., Guha, S., Upadhyay, P. K., & Singh, D. (2023). A Long-Term Analysis of the Dependency of Land Surface Temperature on Land Surface Indexes. Papers in Applied Geography, 9(3). https://doi.org/10.1080/23754931.2023.2187314
27. Panigrahi, M., & Sharma, A. (2025). Urban growth dynamics and its influence on land surface temperature in Bhubaneswar metropolitan city: a 1990–2021 analysis. Discover Applied Sciences, 7(2). https://doi.org/10.1007/s42452-025-06535-y
28. Pathak, C., Chandra, S., Maurya, G., Rathore, A., Sarif, M. O., & Gupta, R. D. (2021). The Effects of Land Indices on Thermal State in Surface Urban Heat Island Formation: A Case Study on Agra City in India Using Remote Sensing Data (1992–2019). Earth Systems and Environment, 5(1). https://doi.org/10.1007/s41748-020-00172-8
29. Putri, R. F., Abadi, A. W., & Tastian, N. F. (2020). Impacts of Population Density for Landuse Assessment in Cengkareng, West Jakarta. Journal of Geoscience, Engineering, Environment, and Technology, 5(2). https://doi.org/10.25299/jgeet.2020.5.2.3705
30. Roy, B., & Kasemi, N. (2021). Monitoring urban growth dynamics using remote sensing and GIS techniques of Raiganj Urban Agglomeration, India. Egyptian Journal of Remote Sensing and Space Science, 24(2). https://doi.org/10.1016/j.ejrs.2021.02.001

31. S, D., K, S., Shanthi Priya, R., & S, R. (2024). Evaluating urban heat island to achieve sustainable development goals: A case study of Tiruchirappalli city, India. Sustainable Cities and Society, 116. https://doi.org/10.1016/j.scs.2024.105865
32. Santhosh, L. G., & Shilpa, D. N. (2023). Assessment of LULC change dynamics and its relationship with LST and spectral indices in a rural area of Bengaluru district, Karnataka India. Remote Sensing Applications: Society and Environment, 29. https://doi.org/10.1016/j.rsase.2022.100886
33. Sarif, M. O., Gupta, R. D., & Murayama, Y. (2023). Assessing Local Climate Change by Spatiotemporal Seasonal LST and Six Land Indices, and Their Interrelationships with SUHI and Hot–Spot Dynamics: A Case Study of Prayagraj City, India (1987–2018). Remote Sensing, 15(1). https://doi.org/10.3390/rs15010179
34. Sarkar, B., Patra, S., & Mishra, M. (2025). Geospatial Analysis of the Relationship Between Land Surface Temperature and Land Use/Land Cover Indices: A Study of Raiganj Municipality, West Bengal, India. Nature Environment and Pollution Technology, 24(2). https://doi.org/10.46488/NEPT.2025.v24i02.B4245
35. Setturu, B., Kumar, U., & Ramachandra, T. V. (2010). Spatio-Temporal Pattern of Landuse Dynamics for Bangalore. Lake 2010: Wetlands, Biodiversity and Climate Change Extents, December.
36. Shahfahad, Kumari, B., Tayyab, M., Ahmed, I. A., Baig, M. R. I., Khan, M. F., & Rahman, A. (2020). Longitudinal study of land surface temperature (LST) using mono- and split-window algorithms and its relationship with NDVI and NDBI over selected metro cities of India. Arabian Journal of Geosciences, 13(19). https://doi.org/10.1007/s12517-020-06068-1
37. Sharma, K., Tiwari, R., Wadhwani, A. K., & Chaturvedi, S. (2024). Spatiotemporal analysis of land surface temperature trends in Nashik, India: A 30-year study from 1992 to 2022. Earth Science Informatics, 17(3). https://doi.org/10.1007/s12145-024-01260-3
38. Sharmita Ghorai (Maity), Ranjit Jana, & Debasish Dasmahapatra. (2024). The scenario of decadal variations in population growth in Purba Medinipur district of West Bengal: A comparative analysis. World Journal of Advanced Research and Reviews, 23(2). https://doi.org/10.30574/wjarr.2024.23.2.2361
39. Sinha, P. N., Patel, N., Jeyaseelan, A. T., & Singh, V. K. (2011). Quantification of Urban Landscape Dynamics Using Patch Parameters and Landscape Indices: An Analytical Study of Ranchi. Journal of the Indian Society of Remote Sensing, 39(2). https://doi.org/10.1007/s12524-011-0068-4
40. Sreenivasulu, V., & Udaya Bhaskar, P. (2010). Change Detection in Landuse and landcover using Remote Sensing and GIS Techniques. International Journal of Engineering Science and Technology, 2(12).
41. Thapa, R., Bahuguna, Dr. V., Negi, P., Rana, P. S., Kataria, P., Rawat, Dr. G., Yasir, M., & Sharma, T. (2023). Examining the spatio-temporal relationship between LST, NDVI, NDBI and LULC change of Pachhua dun, Dehradun, Uttarakhand (India). JGISE: Journal of Geospatial Information Science and Engineering, 6(2). https://doi.org/10.22146/jgise.88002
42. Tiwari, N., Mishra, P. K., & Tripathi, V. K. (2025). Assessment of spatio-temporal variation in seasonal land surface temperature and its relationship with spectral land use indices in Varanasi. Discover Cities, 2(1). https://doi.org/10.1007/s44327-025-00120-z
43. Vanlalchhuanga, Lawmchullova, I., Biswas, B., & Remlalruata. (2025). A study on temporal Land surface temperature (LST) and its relationship with Remote sensing ecological spectral indices of

Agra and Aizawl Cities in India. Journal of Applied and Natural Science, 17(1). https://doi.org/10.31018/jans.v17i1.6360